Large frequency shifts of absorption profiles due to the combination of optical pumping, light shift, and magnetic fields in sodium vapor

B. Röhricht, P. Eschle, C. Wigger, S. Dangel, and R. Holzner
Physik-Institut der Universität Zürich, Winterthurerstrasse 190, CH-8057 Zürich, Switzerland*

D. Suter
Institut für Quantenelektronik, Eidgenössische Technische Hochschule Hönggerberg, CH-8093 Zürich, Switzerland
(Received 8 March 1994)

The absorption profiles of left-hand and right-hand circularly polarized laser light propagating through sodium vapor are asymmetric and considerably frequency shifted if small static magnetic fields are present. Using an analytical model we show how optical pumping "enhances" the laser-induced light shift from the kilohertz to the gigahertz range. We compare the analytical results with experimental data obtained from the homogeneously broadened Na D_1 transition.

PACS number(s): 32.80.Bx, 32.70.Jz, 42.25.Ja, 32.90.+a

INTRODUCTION

The propagation of resonant laser light through nonlinear media usually leads to a modification of optical properties. In this paper we demonstrate and explain such modifications for sodium vapor. The combination of three well-known effects, "optical pumping," "light-shift," and "Larmor precession," can cause a huge apparent frequency shift and asymmetry of the absorption profiles of circularly polarized light near resonant to the atomic D_1 transition which is homogeneously broadened due to collisions between sodium atoms and argon buffer gas.

Optical pumping [1,2], the creation of nonequilibrium population distributions among the spin substates of atoms by resonant light, has been used to investigate fundamental questions of physics for many years [3]. Furthermore it represents an interesting nonlinearity in suitable materials such as alkali vapors since it occurs even at very low light intensities.

Light shift, a shift of energy levels due to optical irradiation, was first discovered by Cohen-Tannoudji and Kastler [4,5] who found shifts of the order of a few hertz using discharge lamps. Light-shift effects produced by moderate laser light intensities are of the order of kHz to MHz and play an important role in various quantum optical systems. By selectively irradiating certain optical transitions, for example, the light-shift effect can be used to manipulate spin dynamics [6,7] and spin-echo phenomena are induced between Zeeman sublevels by pulses of a laser tuned close to an optical resonance [8,9]. Further examples are light-shift-induced chaos in a passive optical cavity [10] and the use of light shifts for quantum nondemolition measurements [11].

Larmor precession due to small transverse magnetic fields causes a reorientation of the atomic magnetization created by optical pumping and therefore changes the population of the magnetic ground-state sublevels.

EXPERIMENT

Experimental evidence for the modification of optical properties by the combined action of these effects is shown in Fig. 1. Both absorption profiles for left-hand (σ_+) and right-hand (σ_-) circularly polarized light are asymmetric and form a mirror image of each other with respect to ω_0, the center frequency of the symmetric ab-

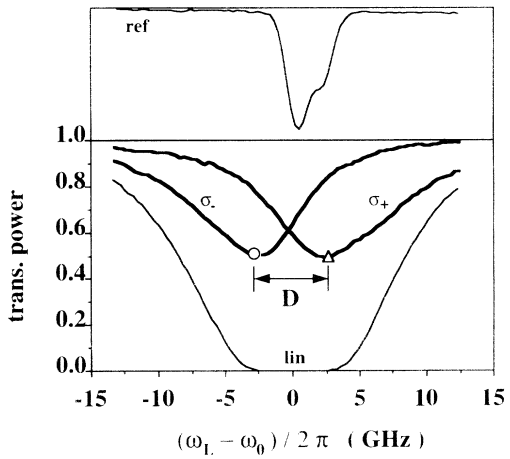

FIG. 1. Experimental absorption profiles in the presence of small static magnetic longitudinal ($B_z = 250$ mG) and transverse ($B_x = 50$ mG) fields for σ_+, σ_- and for linearly polarized laser light after propagation through a Pyrex glass cell containing sodium vapor and argon buffer gas. The symbols △ and ○ indicate positions of minimum transmission of σ_+ and σ_- circularly polarized laser light occurring at frequencies $\omega_{\min}^{+}$ and $\omega_{\min}^{-}$, respectively. $D = (\omega_{\min}^{+} - \omega_{\min}^{-})/2\pi$ is the frequency difference. The reference signal shown on top was obtained by simultaneously passing a small fraction of the input laser beam through a sodium vapor cell without buffer gas.

*Fax: ++41-1-2575704

sorption profile of linearly polarized light (bottom curve). Since all profiles are slightly pressure shifted with regard to the atomic transition without buffer gas (reference signal on top), ω_0 has been taken as the reference for laser-atom detuning. D indicates the separation between frequencies where maximum absorption of σ_+ and σ_- occurs. In the following the shape of the observed absorption profiles is explained qualitatively.

Optical pumping by circularly polarized light between the two magnetic ground-state sublevels $\langle m_j=\frac{1}{2}\rangle$ and $\langle m_j=-\frac{1}{2}\rangle$ of the homogeneously broadened D_1 transition leads to a ground-state magnetization along the laser-beam propagation direction z. External magnetic fields force the magnetization to precess about the direction of the total magnetic field. If the longitudinal magnetic-field component B_z is much larger than the transverse component B_x, the direction of the magnetic field approximately coincides with the direction z of the laser beam propagation. Larmor precession therefore leaves the population of both sublevels $\langle m_j=\frac{1}{2}\rangle$ and $\langle m_j=-\frac{1}{2}\rangle$ almost unchanged. If B_z is reduced to $B_z\approx B_x$ or even $B_z<B_x$, however, the precession of the magnetization causes a significant redistribution of the ground-state sublevel populations which leads to an increased absorption of the circularly polarized pumping beam. In other words, transverse magnetic fields "destroy" the effects of optical pumping while longitudinal magnetic fields "support" optical pumping.

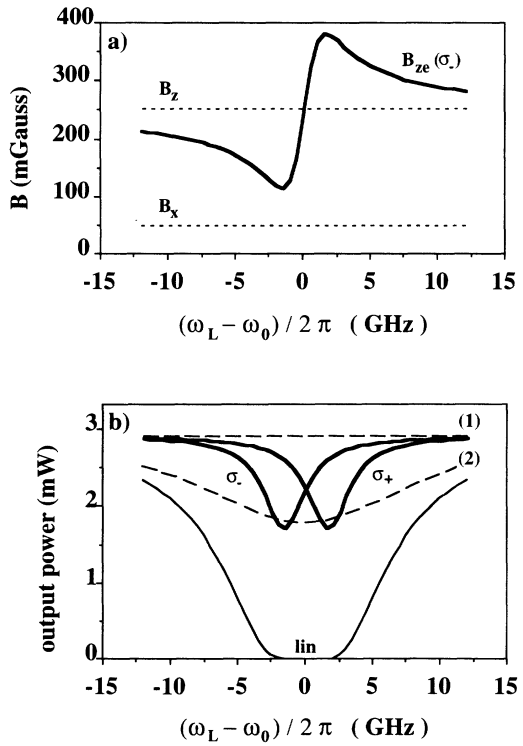

FIG. 2. (a) Calculated total effective longitudinal magnetic field $B_{ze}=B_z+B_{ls}$ for σ_- light as a function of laser-atom detuning. Externally applied transverse and longitudinal magnetic fields are indicated as B_x and B_z. (b) Calculated absorption profiles for circularly polarized light. Dashed line (1): without magnetic fields ($B_{x,z}=0$). Dashed line (2): with transverse magnetic field ($B_x=50$ mG, $B_z=0$). Bold solid lines (σ_+,σ_-): with transverse and longitudinal magnetic fields ($B_x=50$ mG, $B_z=250$ mG). Bottom line (lin): without optical pumping ($R_0=0$, corresponding to linearly polarized light).

The longitudinal magnetic-field component, however, is "modified" by light shift. In the case of circularly polarized light, the effect of the light shift is equivalent to the effect of an intensity and laser frequency-dependent fictitious purely longitudinal static magnetic field B_{ls} [6,7] added to the externally applied constant static field B_z. For σ_- light $B_{ze}=B_z+B_{ls}$ is shown in Fig. 2(a). At negative frequency detunings the effective longitudinal magnetic field component B_{ze} is decreased, which allows the transverse component B_x to destroy optical pumping and therefore to increase absorption. At positive frequency detunings B_{ze} is increased which supports optical pumping and therefore decreases absorption of σ_- light. Maximum absorption therefore occurs close to the laser frequency where B_{ze} has its minimum. For σ_+ light B_{ls} changes sign which leads to a mirror image of the absorption profile for σ_- light as shown in Figs. 1 and 2(b).

The energy-level shifts due to light shift and Zeeman effect are in the range of 1 to 100 kHz which is much less than the homogeneous optical linewidth of about 1.5 GHz due to collisions between sodium and argon buffer gas atoms. Nevertheless one can easily observe a deformation of the absorption profiles leading to large frequency shifts of the absorption maxima due to the combined simultaneous action of optical pumping, light shift, and Larmor precession.

THEORY

For a quantitative analysis of our experimental results we use a simple analytical theory based on a homogeneously broadened $J=\frac{1}{2}$ to $J=\frac{1}{2}$ transition model. We assume a circularly polarized plane wave of uniform intensity for the input laser beam. At laser powers used in the experiment one can neglect excited-state populations and reduce the system to the two substates of the electronic ground state. This quasi-two-state system can be fully described by a spin vector

$$\mathbf{m}=(\rho_{12}+\rho_{21},-i(\rho_{12}-\rho_{21}),\rho_{22}-\rho_{11})\ , \tag{1}$$

where the x and y components represent angular momentum perpendicular to the laser-beam propagation direction, which appear as coherences in the density operator. The z component corresponding to the longitudinal angular momentum is given by the population difference between the two spin substates. This vector evolves under the combined influence of optical pumping, light-shift, and magnetic fields according to the Bloch-type equation of motion [7,10],

$$\dot{\mathbf{m}}=\mathbf{\Omega}\times\mathbf{m}-\gamma_{\text{eff}}\mathbf{m}+\mathbf{R}\ , \tag{2}$$

where Larmor precession occurs about the direction of the total magnetic field given by the vector $\mathbf{\Omega}=\{\Omega_x,\Omega_y,\Omega_z\}$ with $\Omega_x=gB_x$, $\Omega_y=0$, $\Omega_z=\Omega_z'+\Omega_{ls}=gB_z+R\Delta$. g is the gyromagnetic ratio of sodium in the $S_{1/2}$ ground state, B_x the externally applied magnetic

field perpendicular to the laser-beam propagation direction, B_z the externally applied longitudinal magnetic field, and $\Omega_{ls}=R\Delta=gB_{ls}$ the contribution due to light shift [6]. The effective decay rate of the ground-state magnetization $\gamma_{eff}=\gamma_0+R$ consists of a contribution γ_0 due to residual inhomogeneous magnetic fields as well as polarized atoms leaving the beam area, and the optical pump rate $R=R_0/(1+\Delta^2)$ proportional to the laser intensity. $\Delta=(\omega_L-\omega_0)/\Gamma$ is the laser-atom detuning scaled by the optical dipole dephasing rate Γ. Optical pumping is described by $\mathbf{R}=(0,0,R)$.

In the experiments we measure the transmitted power which is determined by Beer's law $P(L)=P_0e^{-\alpha L}$ where L is the length of the cell and

$$\alpha=\alpha_0\rho_{11}\frac{1}{(1+\Delta^2)} \tag{3}$$

is the absorption coefficient. The weak-field resonant absorption coefficient α_0 is proportional to the density of sodium atoms. For simplicity we consider only σ_- light in the following explanations. The population of the ground-state sublevel $\langle m_j=-\frac{1}{2}\rangle$ to which σ_- couples is described by the steady-state solution of (2) for the density operator component ρ_{11} ranging from 0 (no atoms in $\langle m_j=-\frac{1}{2}\rangle$) to $\frac{1}{2}$ (equilibrium population of ground state sublevels without light). The influence of optical pumping, light shift, and magnetic fields on ρ_{11} are therefore described [7] by

$$\rho_{11}=\frac{1}{2}\left[1-\frac{R}{(R+\gamma_0)}\frac{[\Omega_z^2+(R+\gamma_0)^2]}{[\Omega_x^2+\Omega_z^2+(R+\gamma_0)^2]}\right]. \tag{4}$$

The effective longitudinal magnetic field $B_{ze}=\Omega_z/g$ is shown in Fig. 2(a) as a function of detuning.

CALCULATIONS

For the calculations shown in Fig. 2 we used parameter values, which correspond to an experimental setup described in [12,13]: $\alpha_0=548\ \mathrm{m}^{-1}$, $R_0=1.2\times10^6\ \mathrm{s}^{-1}$, $\gamma_0=2.5\times10^3\ \mathrm{s}^{-1}$, $g=2\pi\times7\times10^5\ \mathrm{s}^{-1}\ \mathrm{G}^{-1}$, $P_0=(3\pm1)$ mW input power of σ_+, σ_-, or linearly polarized beams, $w_0=(230\pm10)\ \mu$m beam waist at the input window of the sodium vapor cell, $L=(6.5\pm0.1)$ cm length of the sodium vapor cell, $n_{Na}=(2.5\pm0.5)\times10^{18}\ \mathrm{m}^{-3}$ density of sodium atoms at $T=200\,^\circ$C cell temperature, $n_{Ar}=(8\pm1)\times10^{24}\ \mathrm{m}^{-3}$ density of argon atoms at $p=250$ Torr buffer gas pressure, and $\Gamma=(1.0\pm0.1)\times10^{10}\ \mathrm{s}^{-1}$ optical dipole dephasing rate. For these parameter values $\gamma_0\ll R,\Omega_x,\Omega_z$ is a good approximation which simplifies ρ_{11} in (3) and we obtain

$$\alpha=\tfrac{1}{2}\alpha_0\frac{\Omega_x^2}{[R_0^2+2\Delta R_0\Omega_z'+(1+\Delta^2)(\Omega_x^2+\Omega_z'^2)]}. \tag{5}$$

Maximum absorption therefore occurs at the laser-atom detuning

$$\Delta_{max}=\frac{-R_0\Omega_z'}{(\Omega_x^2+\Omega_z'^2)}. \tag{6}$$

We therefore expect the shift of the absorption maximum to be proportional to the laser-beam intensity and to depend on the longitudinal magnetic field in the same way as a dispersion curve depends on frequency.

EXPERIMENTAL RESULTS AND DISCUSSION

The combination of optical pumping, light shift, and external magnetic fields leads to the shape of the absorption profiles as shown in Figs. 1 and 2(b) for σ_- and σ_+ light. For σ_+ light the optical pumping rate R_0 changes sign in Eqs. (5) and (6). The top curve in Fig. 2(b) represents the case of maximum optical pumping efficiency ($B_x=B_z=0$) and therefore minimum absorption. The full impact of optical pumping is most evident when this curve is compared to the bottom curve. Here the pumping rate R_0 was set to zero which is equivalent to linearly polarized input light. The bold curves show the shifted asymmetric profiles when both $B_x=50$ mG and $B_z=250$ mG are present.

The agreement between experiment and theory is demonstrated in Figs. 3 and 4. The frequency difference $D=(\omega_{min}^+-\omega_{min}^-)/2\pi$ is an antisymmetric function of B_z and remains unaltered upon simultaneous reversal of the field B_z and exchange of σ_+ by σ_-. The dependence of the frequency difference D on the input laser beam power is shown in Fig. 4. D increases sharply up to about $P_0=10$ mW before it decreases again at larger input powers. There the light-shift contribution dominates all other magnetic fields and affects both σ_+ and σ_- absorption profiles almost symmetrically. The predicted linear dependence (6) of Δ_{max} on the input power breaks down since even a small γ_0 can become important if R_0 is large. The theoretical curve was therefore obtained by numerically evaluating (3).

The qualitative agreement between experiment and our model is satisfying. In order to obtain good quantitative agreement as shown in Fig. 4, we used a value for the ground-state magnetization decay rate of $\gamma_0=4.7\times10^4\ \mathrm{s}^{-1}$ for the calculations. This value is about one order of

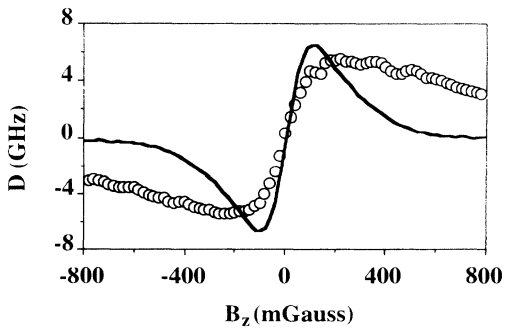

FIG. 3. Frequency difference D between minima of absorption profiles for σ_+ and σ_- radiation as a function of the externally applied magnetic field B_z at constant transverse magnetic field $B_x=50$ mG. Solid line: theory; ○: experiment.

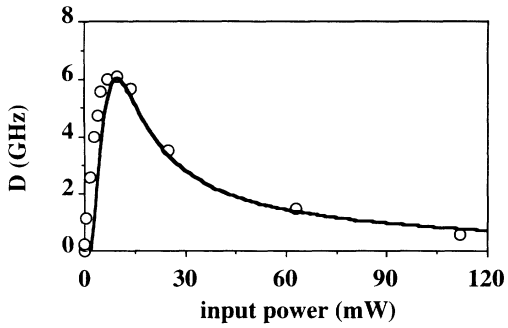

FIG. 4. Frequency difference D between minima of absorption profiles for σ_+ and σ_- radiation as a function of input beam power at $B_z=200$ mG and $B_x=50$ mG. Solid line: theory; ○: experiment.

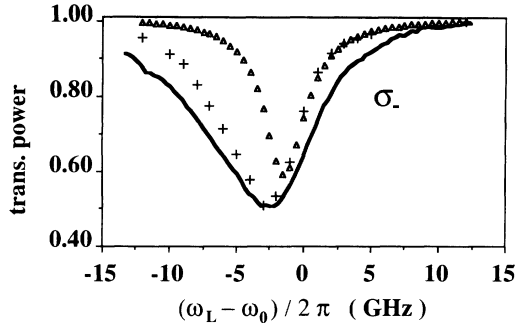

FIG. 5. Comparison of experiment (solid line) with numerical calculations from the full wave equation model (+) and our simple theory (Δ). Parameter values for the full model and the simple theory [see Fig. 2(b)] were chosen identical. They are within the uncertainty limits of the experimental values which correspond to the absorption profiles shown in Fig. 1.

magnitude larger than the value $\gamma_0=2.5\times10^3$ s^{-1} estimated from a random-walk-type diffusion of Na atoms in buffer gas.

Remaining differences between experiment and model may be due to approximations which do not account for laser light propagation effects (e.g., self-focusing and defocusing), the Gaussian transverse intensity distribution of the laser beam nor the nonuniform intensity distribution along the cell. Furthermore the model assumes the magnetic fields to be homogeneous whereas we measured residual ac and dc magnetic stray fields of about ±3 mG along the beam path through the cell, using a 3-axis magnetic-field sensor (MAG-03-MC from Bartington). Some of these differences can be removed when the full model [14,12] is used. This semiclassical model does include saturation, diffraction, optical pumping, and beam propagation effects and therefore fully accounts for the Gaussian intensity distribution of the laser beams as well as for the nonuniform intensity distribution along the sodium cell. The comparison between experimental data, simplified analytic model, and numerical solutions from the semiclassical wave equation model is shown in Fig. 5 for the σ_- absorption profile. All three profiles show about equal maximum absorption at approximately the same laser frequency. The width of the absorption profile is smallest for the analytic model whereas the semiclassical model approaches the experimental curve considerably better.

CONCLUSIONS

We have reported experimental results demonstrating that the shape of absorption profiles may depend on the polarization of the light propagating through a homogeneously broadened nonlinear medium. For the Na D_1 transition, we have found shifts of several GHz which depend on the light intensity and on external magnetic fields. Using a simple analytical model, we have shown that the effects are due to a combination of optical pumping, light-shift effects, and Larmor precession. Since the behavior of the system is highly nonlinear, the combination of these effects results in shifts that are, under typical experimental conditions, five orders of magnitude larger than the Zeeman and light-shift effects alone. Since measuring absorption profiles is a standard procedure in laser physics, we believe that the consideration of such absorption profile shifts is important if small magnetic fields are present.

ACKNOWLEDGMENTS

We would like to thank A. W. McCord for his help with the numerical treatment of the semiclassical laser beam propagation model and the "Schweizerischer Nationalfonds" as well as the "ErnstHadorn Stiftung" for financial support.

[1] A. Kastler, J. Opt. Soc. **47**, 460 (1957).
[2] W. Happer, Rev. Mod. Phys. **44**, 169 (1972).
[3] R. J. Knize, Z. Wu, and W. Happer, in *Advances in Atomic and Molecular Physics,* edited by D. Bates and B. Bederson (Academic, New York, 1988), pp. 223–267.
[4] C. Cohen-Tannoudji, Ann. Phys. (Paris), **7**, 423 (1962).
[5] A. Kastler, Science **158**, 214 (1967).
[6] C. Cohen-Tannoudji and J. Dupont-Roc, Phys. Rev. A **5**, 968 (1972).
[7] D. Suter and J. Mlynek, Adv. Magn. Opt. Res. **16**, 1 (1992).
[8] M. Rosatzin, D. Suter, and J. Mlynek, Phys. Rev. A **42**, 1839 (1990).
[9] D. Suter, M. Rosatzin, and J. Mlynek, Phys. Rev. Lett. **67**, 34 (1991).
[10] C. Boden, M. Dämmig, and F. Mitschke, Phys. Rev. A **45**, 6829 (1992).
[11] M. Brune, S. Haroche, V. Lefevre, J. M. Raimond, and N. Zagury, Phys. Rev. Lett. **65**, 976 (1990).
[12] R. Holzner, P. Eschle, A. W. McCord, and D. M. Warrington, Phys. Rev. Lett. **69**, 2192 (1992).
[13] B. Röhricht, P. Eschle, S. Dangel, and R. Holzner, Z. Naturforsch. Teil A **48**, 621 (1993).
[14] A. W. McCord and R. J. Ballagh, J. Opt. Soc. Am. B **7**, 73 (1990).